Mixtures of Cationic Lipid *O*-Ethylphosphatidylcholine with Membrane Lipids and DNA: Phase Diagrams

Rumiana Koynova and Robert C. MacDonald
Department of Biochemistry, Molecular Biology and Cell Biology, Northwestern University, Evanston, Illinois USA

ABSTRACT Ethylphosphatidylcholines are positively charged membrane lipid derivatives, which effectively transfect DNA into cells and are metabolized by the cells. For this reason, they are promising nonviral transfection agents. With the aim of revealing the kinds of lipid phases that may arise when lipoplexes interact with cellular lipids during DNA transfection, temperature-composition phase diagrams of mixtures of the *O*-ethyldipalmitoylphosphatidylcholine with representatives of the major lipid classes (phosphatidylcholine, phosphatidylethanolamine, phosphatidylglycerol, cholesterol) were constructed. Phase boundaries were determined using differential scanning calorimetry and synchrotron x-ray diffraction. The effects of ionic strength and of DNA presence were examined. A large variety of polymorphic and mesomorphic structures were observed. Surprisingly, marked enhancement of the affinity for nonlamellar phases was observed in mixtures with phosphatidylethanolamine and cholesterol as well as with phosphatidylglycerol (previously reported). Because of the potential relevance to transfection, it is noteworthy that such phases form at close to physiological conditions, and in the presence of DNA. All four mixtures exhibit a tendency to molecular clustering in the gel phase, presumably due to the specific interdigitated molecular arrangement of the *O*-ethyldipalmitoylphosphatidylcholine gel bilayers. It is evident that a remarkably broad array of lipid phases could arise in transfected cells and that these could have significant effects on transfection efficiency. The data may be particularly useful for selecting possible "helper" lipids in the lipoplex formulations, and in searches for correlations between lipoplex structure and transfection activity.

INTRODUCTION

In recent years, it has become apparent that lipidlike compounds can be used to deliver DNA to cells, a procedure that may become clinically important (see e.g., Felgner and Ringold, 1989; Zhu et al., 1993; Felgner, 1997). The molecules that are most efficient in delivering DNA to cells are positively charged amphiphiles, and such cationic compounds are now being intensively studied. Because of their potential application in gene therapy, and probably also because of drug delivery applications, interest in cationic lipidlike molecules has grown explosively. There are many lipoplex preparations available currently, and a host of cationic lipoids have been used in their formulation. A large variety of such compounds has been synthesized and tested, and although described as ''cationic lipids,'' they are not natural products but rather are almost always cationic amphiphiles or detergents, i.e., synthetic compounds that are physically similar but chemically different from natural polar lipids. In fact, phosphatidylcholine triesters (MacDonald et al., 1999a,b; Rosenzweig et al., 2000; Solodin et al., 1996; see also this article, Fig. 1) are lipid derivatives and, to date, the only cationic amphipaths shown to be metabolized by cells.

Submitted May 5, 2003, and submitted for publication July 16, 2003.

Rumiana Koynova is also an Associated Member of the Institute of Biophysics, Bulgarian Academy of Sciences.

Address reprint requests to Rumiana Koynova, Dept. of Biochemistry, Molecular Biology, and Cell Biology, Northwestern University, 2205 Tech Dr., Evanston, IL 60208. Tel.: 847-491-2871; Fax: 847-467-1380; E-mail: r-tenchova@northwestern.edu.

0006-3495/03/10/2449/17 $2.00

Aqueous dispersions of polar lipids are known for their ability to form a large variety of polymorphic and mesomorphic phases (see, e.g., Lipid Data Bank, LIPIDAT, http://www.lipidat.chemistry.ohio-state.edu). Although the majority of cationic lipids used for transfection arrange themselves into lamellar phases, it has been shown that their mixtures with other lipids (so-called helper lipids, introduced to improve transfection efficiency) are also able to form the inverted hexagonal phase, and even to incorporate DNA within it (Koltover et al., 1998; Rakhmanova et al., 2000). Correlations between the mesomorphic phase state of the lipoplexes and their transfection activity have been sought, but so far there is no clear consensus as to whether the nonlamellar phases per se are beneficial for transfection (Koltover et al., 1998; Rakhmanova et al., 2000; Zuhorn et al., 2002; Zuhorn and Hoekstra, 2002), even though the issue remains of interest.

The topic of the phase behavior of the mixtures of cationic lipids with other polar lipids is important not only from the viewpoint of the possible use of helper lipids and their effect on lipoplex structure and activity, but also as an attempt to assess the lipid phases that may arise when cationic lipids of the lipoplexes interact with cellular lipids during DNA transfection. It was recently shown that mixtures of cationic and anionic lipids form nonlamellar phases in the composition region close to charge neutrality, although the pure components form only lamellar phases (Tarahovsky et al., 2000; Lewis and McElhaney, 2000). This propensity could be important in the process of DNA delivery by amphipathic cationic vectors (Zuhorn and Hoekstra, 2002).

Here we present the detailed temperature-composition phase diagrams of the cationic phospholipid *O*-ethyldi-

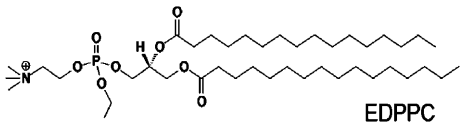

FIGURE 1 Molecular structure of 1,2-dipalmitoyl-*sn*-glycero-3-ethylphosphocholine (EDPPC).

palmitoylphosphatidylcholine (EDPPC) in mixtures with representatives of the major cellular lipid classes—phosphatidylcholine, phosphatidylethanolamine, phosphatidylglycerol, and cholesterol, constructed by means of differential scanning calorimetry (DSC) and small-angle x-ray diffraction (SAXD). Corresponding phase diagrams of these mixtures in the presence of DNA are also presented. With regard to understanding the interactions controlling lipid phase energetics it is interesting that this cationic lipid either generated or strongly enhanced the propensity for nonlamellar phase formation not only in mixtures containing the anionic phosphatidylglycerol, but also in those containing phosphatidylethanolamine and cholesterol. For the first time, nonlamellar liquid crystalline phases (cubic, inverted hexagonal) are described in mixtures of the cationic ethylphosphatidylcholine with phosphatidylethanolamine and cholesterol, and with phosphatidylglycerol in the presence of DNA. Obviously, an unusually broad array of lipid phases could arise in transfected cells. Also, these results imply that a larger set of potential helper lipids could be considered in lipoplex transfection formulations.

MATERIALS AND METHODS

Lipids

The triflate derivative of dipalmitoyl ethylphosphatidylcholine (EDPPC) was synthesized as previously described (MacDonald et al., 1999a,b; Rosenzweig et al., 2000). In some experiments, the chloride salt of EDPPC from Avanti Polar Lipids (Birmingham, AL) was used. 1,2-dipalmitoyl-*sn*-glycero-3-phosphocholine (DPPC), 1,2-dielaidoyl-*sn*-glycero-3-phosphoethanolamine (DEPE), 1,2-dipalmitoyl-*sn*-glycero-3-[phospho-*rac*-(1-glycerol)] (sodium salt) (DPPG) from Avanti Polar Lipids (Birmingham, AL), and cholesterol from Sigma (Sigma-Aldrich, St. Louis, MO) were used without further purification. The phospholipids were found to migrate as a single spot by thin-layer chromatography. Microcalorimetric scans of their diluted dispersions showed highly cooperative chain-melting phase transitions at temperatures in agreement with published values. Lipids were stored at −20°C in chloroform. Aliquots were transferred to vials where the bulk of the solvent was removed with a stream of argon. The vial was then placed under high vacuum for at least 1 h/mg lipid, to remove residual chloroform. Next, the appropriate aqueous medium was added—either deionized water from a Millipore Milli-Q water system, or PBS (50 mM Na_2HPO_4, 100 mM NaCl, brought to pH 7.2 with 100 mM HCl). The dispersions were hydrated overnight at 4°C, then heated to 50°C and vortex-mixed at that temperature for several minutes. Samples were equilibrated at 4°C for 1–3 days before measurements. Lipid concentrations of stock solutions were determined using a phosphate assay (Bartlett, 1959). The lipid concentration of the dispersions was 1–3 mg/ml for calorimetry, and 5–25 wt % for x-ray diffraction. For x-ray measurements, samples were filled into glass capillaries ($d = 1.0$ or 1.5 mm) (Charles Super Company, Natick, MA) and flame-sealed with a butane microtorch.

DNA

Herring sperm DNA (Invitrogen, Carlsbad, CA), 10 mg/ml solution in water, was used. The amount of DNA in the lipoplex samples was intended to match the positive charge of the cationic lipid, assuming an average nucleotide mol wt 330 (isoelectric samples). DNA/lipid dispersions for calorimetry were prepared by adding the DNA solution drop-wise to the preformed lipid dispersions. Samples were equilibrated for 1–3 days at room temperature before measurements. For x-ray samples, 5 wt % lipid dispersions were sonicated to near-clarity at temperature 5–10°C above the chain melting transition, DNA was added, and the suspensions were equilibrated overnight. The samples were concentrated either by centrifugation or by lyophilization and rehydration. After sealing into capillaries, samples were temperature-cycled several times between 50°C and room temperature, and equilibrated for 5–7 days at room temperature before measurements. Test samples equilibrated with DNA for longer times (up to 20 days) displayed unaltered diffraction patterns and DSC thermograms.

Differential scanning calorimetry

High-sensitivity microcalorimetric measurements were performed with a VP-DSC Microcalorimeter (MicroCal, Northampton, MA; see also Plotnikov et al., 1997). Heating and cooling scans were at rates of 0.2–0.5°C/min (4-s filtering). Thermograms were analyzed using Origin Labs (Northampton, MA) software. The onset and the completion temperatures of the phase transitions necessary for the construction of the phase diagram were determined by the intersections of the peak slopes with the baseline on the thermograms. The phase diagrams have been corrected for the finite width of the transitions of the pure components (Lee, 1977).

Synchrotron small-angle x-ray diffraction (SAXD) measurements

SAXD measurements were performed at Argonne National Laboratory, Advanced Photon Source, DND-CAT (beamline 5-IDD) and BioCAT (beamline 18-ID). At DND-CAT, 15 keV x-rays were used; data were collected using a MAR-CCD detector (165-mm diameter, 2048 × 2048 pixels, 78.75 μm pixel size, 300 × 300-μm beam size). At BioCAT, 12 keV x-rays were used; two-dimensional diffraction patterns were recorded using a high-sensitivity CCD detector (Phillips et al., 2002) (50 × 90 mm, 1028 × 1798 pixels, 48-μm pixel size, beam size at the CCD surface 50 × 150 μm). Sample-to-detector distance was 1.8–2 m. Silver behenate (DuPont, Wilmington, DE) was used as a calibrant ($d_{001} = 58.376$ Å; see Blanton et al., 1995). For temperature control, either a THMS600 thermal stage (Linkam Scientific Instruments, Surrey, UK), or a NESLAB programmable water bath (Thermo NESLAB, Portsmouth, NH) was used. Linear heating and cooling scans were performed at rates of 0.8–3°C/min. Exposure times were typically 0.5–5 s. The two-dimensional diffraction patterns did not show angular dependence of the scattered intensity for the phases studied. Diffraction intensity vs. reciprocal space *s*-plots were obtained by radial integration of the two-dimensional patterns using the interactive data-evaluating program FIT2D (Hammersley, 1998; Hammersley et al., 1996). Some samples with longer exposure time were checked by thin layer chromatography after the experiments. Products of lipid degradation were not detected in these samples, and radiation damage of the lipids was not evident from their x-ray patterns.

RESULTS AND DISCUSSION

DPPC/EDPPC

A selection of calorimetric thermograms of aqueous dispersions of mixtures of EDPPC and DPPC at different

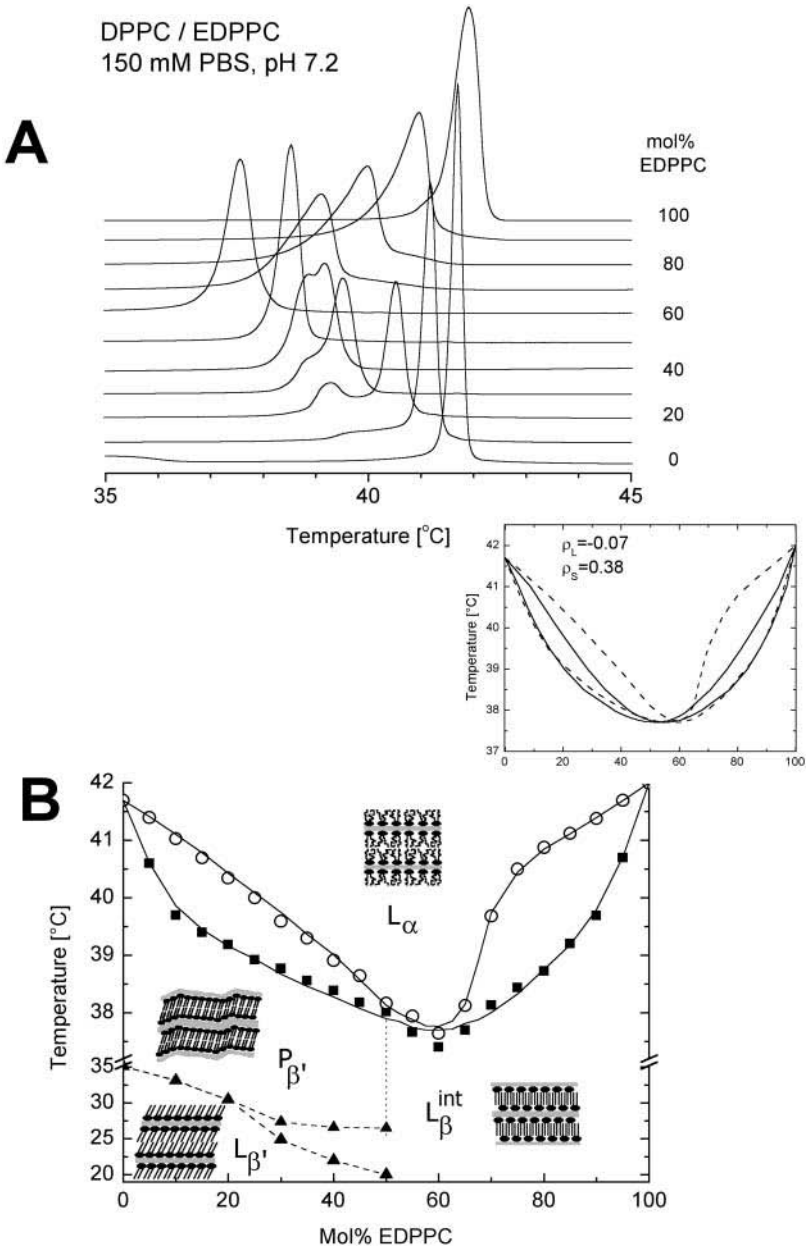

FIGURE 2 DPPC/EDPPC pseudobinary mixture in PBS, pH 7.2. (*A*) DSC heating thermograms at different compositions (0.5°C/min scan rate). (*B*) Temperature-composition phase diagram: *solidus* line (*solid squares*); *liquidus* line (*open circles*); and pretransition (*solid triangles*). Between 20 and 50 mol % EDPPC, the pretransition splitting is suggestive of the induction of interdigitated gel phase between the $L_{\beta'}$ and the rippled $P_{\beta'}$ phases, similar to the aqueous DPPC/ethanol mixture, in which conversion from noninterdigitated to interdigitated gel phase also takes place upon change of composition (Simon and McIntosh, 1984; Nambi et al., 1988; Ohki et al., 1990). (*Inset*) Theoretical simulation of the DPPC/EDPPC phase diagram at nonideal parameters: $\rho_S = 0.38$ kT, $\rho_L = -0.07$ kT (*solid line*); experimental phase diagram (*dashed line*).

mole ratios is shown in Fig. 2 *A*. Pure hydrated EDPPC exhibited a melting transition at $T_m = 42$°C, with enthalpy change of 9.6 kcal/mol, in agreement with previous reports (MacDonald et al., 1999a; Lewis et al., 2001; Winter et al., 2001). EDPPC was chosen for the present study because its phase transition is in convenient temperature range. It is worth noting that although at physiological temperatures it is in the gel phase, it still transfects DNA into cells, provided the lipoplexes are formed at $T > T_m$ (Wang, L., et al., unpublished observation). (Note: In fact, reports exist that gel-phase liposomes adsorb better onto solid surfaces (Tenchov et al., 1989) and associate better with cells (Mincheva et al., 1990) than the liquid crystalline liposomes.) The melting transition of the hydrated DPPC was at $T_m = 41.7$°C, 7.9 kcal/mol, as reported (Lipid Data Bank, LIPIDAT, http://www.lipidat.chemistry.ohio-state.edu; see also Koynova and Caffrey, 1998). The melting transition temperatures for the mixtures were lower than those of the pure compounds for all compositions, with a minimum at 60 mol % EDPPC, where it was 37.5°C. The pretransition ($L_{\beta'} \rightarrow P_{\beta'}$ transition), characteristic of the DPPC dispersions, also decreased in temperature with increasing EDPPC content, split at >20 mol % EDPPC, and disappeared from the thermograms at >50 mol % EDPPC.

The phase diagram constructed on the basis of the calorimetric results is depicted in Fig. 2 *B*. It is presented as a binary temperature-composition phase diagram. The third component—water—is considered to be well above the

excess limit and thus without influence on the properties of the mixtures. This is the conventional approach in studying hydrated lipid mixtures (Chernik, 1995). The DPPC/EDPPC phase diagram is characterized by a low-temperature isoconcentration (azeotropic) point at 60 mol % EDPPC and 37.5°C.

Azeotropic phase diagrams have been previously reported for other lipid mixtures containing charged lipids (e.g., Silvius, 1991; Linseisen et al., 1996; Garidel et al., 1997; Zantl et al., 1999). Typically, however, these were all phase diagrams of the upper isoconcentration point type, in which the transition temperatures of the mixtures are higher than those of the pure components and exhibit maxima at particular compositions. Simulations of the phase lines according to the regular solution approximation show that such phase diagrams with upper isoconcentration points typically reflect higher values of the excess free energy of mixing (''nonideal'' energy) in the liquid than in the solid state (Gordon, 1968). Such a combination of nonideal energies is easily conceivable in mixtures with negative nonideal energy in the solid state, in which contacts between unlike molecules are preferred to those between like ones, i.e., when the nearest-neighbor pairs tend to be made up of unlike molecules. Minimization of the electrostatic repulsion in some mixtures containing charged components could certainly result in such a tendency.

In contrast to the previously described lipid mixtures containing charged lipids, the DPPC/EDPPC binary mixture has a phase diagram that is of the lower isoconcentration point type. Since such phase diagrams are rare in the lipid systems, we tried to simulate it within the regular solution approximation, as previously described (Koynova et al., 1987). Our best-fit result (Fig. 2, *inset*) was with $\rho_L = -0.07$ kT, and $\rho_S = 0.38$ kT, where ρ is the so-called nonideal parameter: $\rho = Z \times E_{non}/2$, Z is the first coordination number (number of nearest neighbors on the lattice), and the nonideal energy $E_{non} = 2E_{AB}\text{-}E_{AA}\text{-}E_{BB}$, where E_{AA}, E_{BB}, and E_{AB} are the interaction energies of the three kinds of nearest neighbor pairs. Such a nonideal parameter accounts for the nonideal enthalpy contribution to the excess free energy of mixing: $\Delta H_{mix} = \rho \times X_A X_B$, with X_A and X_B being the molar fraction of components A and B (Lee, 1977). Subscripts S and L stand for the solid and liquid crystalline phase, respectively.

Due to the simplicity of the approximation used (the applied nonideality correction contributes only to the enthalpy term in the free energy of mixing, whereas the mixing entropy remains equal to that of an ideal mixture), it can hardly be expected to be satisfactory in a quantitative way. Another limitation of that approximation is that it implies a constant nonideal energy for all compositions. Nevertheless, it has been frequently applied to the analysis of lipid phase diagrams (e.g., Lee, 1977; Tenchov, 1985; Inoue et al., 1992, and references therein) and has been found to predict correctly the general qualitative features observed in binary mixtures (Hill, 1960). Thus, for the DPPC/EDPPC mixture, the system appears to be homogeneous in the gel and liquid crystalline phases at all compositions, and to exhibit some clustering of the lipids of the same type in the gel phase ($\rho_S = 0.38$ kT). Mixing in the liquid crystalline phase is virtually ideal ($\rho_L = -0.07$ kT). Parenthetically, the gel phase mixing is also close to ideal—for comparison, the estimated gel phase nonideal parameter ρ_S for the DMPC/DPPC mixture, which is considered of rather good mixing itself, is $\sim 4\times$ bigger than that for DPPC/EDPPC (Lee, 1978). With these estimated nonideal parameters for the DPPC/EDPPC binary, a ''mixing'' contribution of $<1\%$ (0.06 kcal/mol) would be expected to add to the melting enthalpy of the 60 mol % EDPPC (azeotropic) sample—a value which is within the error limit of the enthalpy measurement. A quantitative idea about the degree of clustering is possible within another statistical mechanical approximation, the quasichemical, in which the mixing entropy is not taken to be equal to that of an ideal mixture (Hill, 1960; von Dreele, 1978). Given that the nonideal energies estimated by using the regular solution and the quasichemical approximations are usually quite similar (Tenchov et al., 1984; Koynova et al., 1987), we used the value of the nonideal energy in the solid phase obtained from the former approximation: $E^S_{non} = 2\rho_S/Z = 0.127$ kT (for $Z = 6$), to roughly estimate the degree of clustering using the equations of the quasichemical one (von Dreele, 1978). Thus calculated, the decrease of the number of mixed nearest-neighbor pairs as compared to the ideal mixing in the solid phase of the DPPC/EDPPC mixture at the azeotropic composition (60 mol % EDPPC) is 3%, i.e., the lipid mixing even in the gel phase of the DPPC/EDPPC binary is close to ideal.

The tendency to clustering in the solid phase, despite what could be expected on purely electrostatic grounds, is possibly a result of the major difference in the gel phase packings of the two lipids: whereas EDPPC molecules arrange in an interdigitated gel phase (favorable for optimizing the van der Waals interactions between the hydrophobic chains and simultaneously accommodating the effectively bigger, electrically charged headgroups), DPPC forms a noninterdigitated gel phase with tilted hydrocarbon chains. To test this assumption, it is instructive to compare the mixing properties of this lipid pair with another pair of similar lipids, DPPC and DHPC, which exhibit the same difference in their gel phase arrangements, because DHPC, the ether analog of DPPC, also forms an interdigitated gel phase (Laggner et al., 1987; Kim et al., 1987a). For both lipids, DPPC and DHPC, the transition to the liquid crystalline phase is mediated by the formation of a rippled gel P_β phase, and thus at the rippled-to-liquid crystalline phase transition, the mixture is close to ideal. The transition from the lamellar gel to the rippled phase for mixtures of different compositions, on the other hand, exhibits azeotropic behavior, similar to the melting transition of the DPPC/EDPPC mixtures, with a minimum isoconcentration

point at DPPC/DHPC 1:1 ratio (Lohner et al., 1987; Kim et al., 1987b). In another phosphatidylcholine mixture, dimyristoylphosphatidylcholine (DMPC) and 1-stearoyl-2-capryl phosphatidylcholine (18:0/10:0 PC), a similar major disparity in the gel phase packing arrangements of the two components—interdigitated for 18:0/10:0 PC vs. noninterdigitated, tilted, for DMPC—has been shown to result in extended regions of phase separation in the gel phase and a eutectic phase diagram (Lin and Huang, 1988). In the DPPC/EDPPC mixture, the electrostatic interactions counteract the steric tendency to phase separation and the system is homogeneous even though the analysis of the phase diagram reveals that some clustering in the gel phase persists.

We also performed small-angle x-ray diffraction (SAXD) measurements on DPPC/EDPPC mixtures. They were found to form lamellar phases over the whole temperature/composition space studied. Phase coexistence was observed only within the transition region, whereas outside it both gel and liquid crystalline phases were homogeneous, as expected from the shape of the phase diagram. The lamellar repeat distances as a function of temperature are shown in Fig. 3, and as a function of composition in the gel (20°C) and liquid crystalline (50°C) phases, in Fig. 4. According to these data, the chain interdigitation characteristic for the EDPPC bilayers is preserved up to at least 70 mol % DPPC, i.e., addition of not more than 30 mol % EDPPC is enough to induce interdigitation in the DPPC gel phase. For comparison, the borderline between interdigitated and noninterdigitated gel phase in the mixture DPPC/DHPC is at 1:1 mol ratio (Lohner et al., 1987), i.e., the cationic EDPPC is particularly effective in promoting chain interdigitation since both electrostatic repulsion and bulky headgroup favor interdigitation. In the liquid crystalline phase, as little as 20 mol % DPPC considerably increased the lamellar repeat—from 53 Å for the pure EDPPC, up to 62.5 Å. A maximum in the lamellar repeat was observed at ~40 mol % DPPC.

The above measurements were in buffer at physiological electrolyte concentration (PBS, pH 7.2). For comparison, we performed DSC measurements of DPPC/EDPPC mixtures in water, and also in the presence of an isoelectric amount of DNA. The phase diagrams constructed from these DSC data are shown in Fig. 5. The phase diagram in water (Fig. 5 *A*) is characterized by a combination of lower and upper isoconcentration points, at ~20 mol % and 65 mol % EDPPC, respectively. The difference between this phase diagram and that of Fig. 2 *B* is a result of the absence of salts to screen the charge of the lipid molecules—its greater complexity likely reflects the juxtaposition and delicate balance of electrostatic interactions tending to separate like molecules, and steric interactions tending to cluster them together. Thus, at lower EDPPC concentrations, the gel phase packing differences dominate and the like lipid molecules tend to cluster together, giving rise to a lower isoconcentration point; at >50 mol % EDPPC the electrostatic interactions dominate and the mixing is closer to ideal, with apparently even a slight preference to unlike neighbors in the gel phase that results in an upper isoconcentration point. A similar complex phase diagram comprising lower and upper isoconcentration points (at low and high contents of the charged component, respectively) has been constructed for another mixture involving the charged lipid, *n*-biotinylphosphatidylethanolamine (Swamy et al., 1995).

In the presence of an isoelectric amount of DNA, the phase diagram of the DPPC/EDPPC mixture is similar to that in physiological salt solution, slightly shifted toward the lower EDPPC concentrations, with a lower isoconcentration point

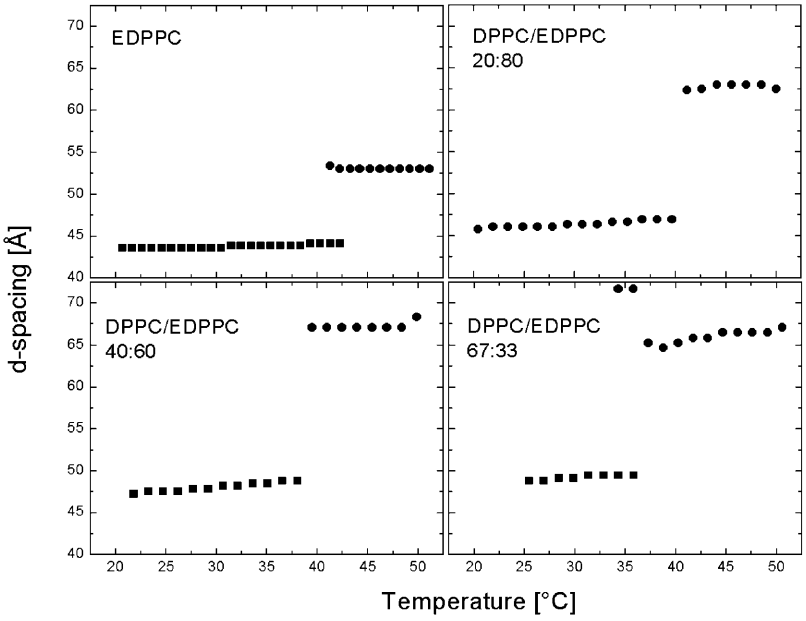

FIGURE 3 DPPC/EDPPC mixture in PBS, pH 7.2. Lamellar repeat distances of samples of different composition, as determined from SAXD experiments (the high lamellar repeat period, ~72 Å, observed in the 67:33 DPPC/EDPPC sample at ~35°C presumably reflects the appearance of a rippled gel phase between the interdigitated gel and the liquid crystalline phases).

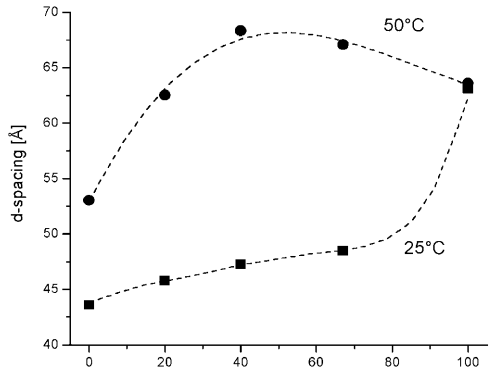

FIGURE 4 DPPC/EDPPC mixture in PBS, pH 7.2. Lamellar repeat distances at 25°C and 50°C as a function of composition.

at 40 mol % EDPPC and 38.5°C (Fig. 5 *B*). The existence of a horizontal portion of the *solidus* line at 25–35 mol % EDPPC, indicating a limited phase separation region in the gel phase, could not be excluded. Clearly, the presence of DNA reduces the electrostatic interactions between the lipid layers, similarly to the salts.

DEPE/EDPPC

In Fig. 6 *A*, a selection of DSC thermograms of EDPPC/DEPE mixtures in PBS (pH 7.2) is presented. The transition enthalpies determined from those thermograms are shown in Fig. 6 *B*. Pure DEPE dispersions displayed a gel-liquid crystalline melting transition at 37.2°C, and a lamellar-inverted hexagonal mesomorphic transition at 63.4°C, in agreement with published data (for a review, see Koynova and Caffrey, 1994). With increasing EDPPC, the main transition temperature decreased, and, at 40 mol % EDPPC, a cooperative endotherm at 28°C was observed. The same endotherm could be distinguished in the thermograms at up to 90 mol % EDPPC. A second endotherm appeared and increased in temperature as the EDPPC fraction was increased above 40 mol %—from 28°C at 40 mol % EDPPC to 42°C at 100% EDPPC. The $L_\alpha \rightarrow H_{II}$ transition of DEPE could not be detected on the thermograms in the presence of EDPPC. Small heat capacity anomalies were observed in the thermograms of the samples with high contents of DEPE at temperatures above the melting transition, not with a reliable reproducibility.

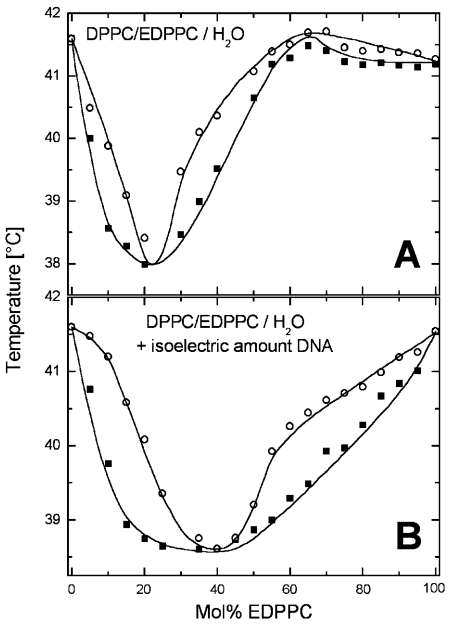

FIGURE 5 Temperature-composition phase diagrams of DPPC/EDPPC mixture in H_2O (*A*), and the presence of isoelectric amount of DNA (*B*), as determined from DSC measurements.

The constructed phase diagram, corrected for the finite width of the pure component phase transitions, is shown in Fig. 6 *C*. It is a eutectic phase diagram, with a eutectic point at 40 mol % EDPPC and a eutectic horizontal at 28°C. According to its shape, there is continuous mixing at all compositions in the liquid crystalline phase. In the gel phase, the lipids mix at up to ~30 mol % EDPPC. The horizontal *solidus* line for EDPPC mol % between 30 and 90 indicates gel phase immiscibility in that composition region, i.e., aggregates with ~2:1 DEPE/EDPPC stoichiometry coexist with almost pure EDPPC aggregates <28°C. Their relative amount is determined according to the lever rule (Gordon, 1968). Upon reaching 28°C, the sample with 40 mol % EDPPC melts quasi-isothermally into a homogeneous liquid crystalline phase (the system is, in fact, pseudobinary, inasmuch as water and salt are present as additional components). In contrast, temperature regions of gel-fluid phase coexistence are anticipated in the samples of lower and higher EDPPC content before transforming into homogeneous liquid crystalline phase.

Similarly to the DPPC/EDPPC mixture discussed above, there is a major difference in the gel phase packing arrangement of EDPPC and DEPE—interdigitated vs. noninterdigitated—which impedes the gel phase mixing. The difference of the headgroups is an additional reason for the contacts between like-molecules to be preferred in this mixture. This is supported by the data of Sisk and Huang (1992) for another lipid system with a similar chain packing disparity—diheptadecanoyl phosphatidylethanolamine (17:0/17:0 PE) and 1-behenoyl-2-lauroylphosphatidylcholine (22:0/12:0 PC). The progressive demethylation of the headgroup of the diheptadecanoyl compound, from phosphocholine to phosphoethanolamine, resulted in considerable increase of the gel phase immiscibility—to virtually the entire compositional range (Sisk and Huang, 1992). With the DEPE/EDPPC system, the immiscibility region is limited to 30–90 mol % EDPPC.

SAXD patterns of DEPE/EDPPC samples at 0, 20, 40, 70, and 100 mol % EDPPC were recorded using a synchrotron x-ray source. This method was particularly suitable to the present study because it provided sufficiently high time

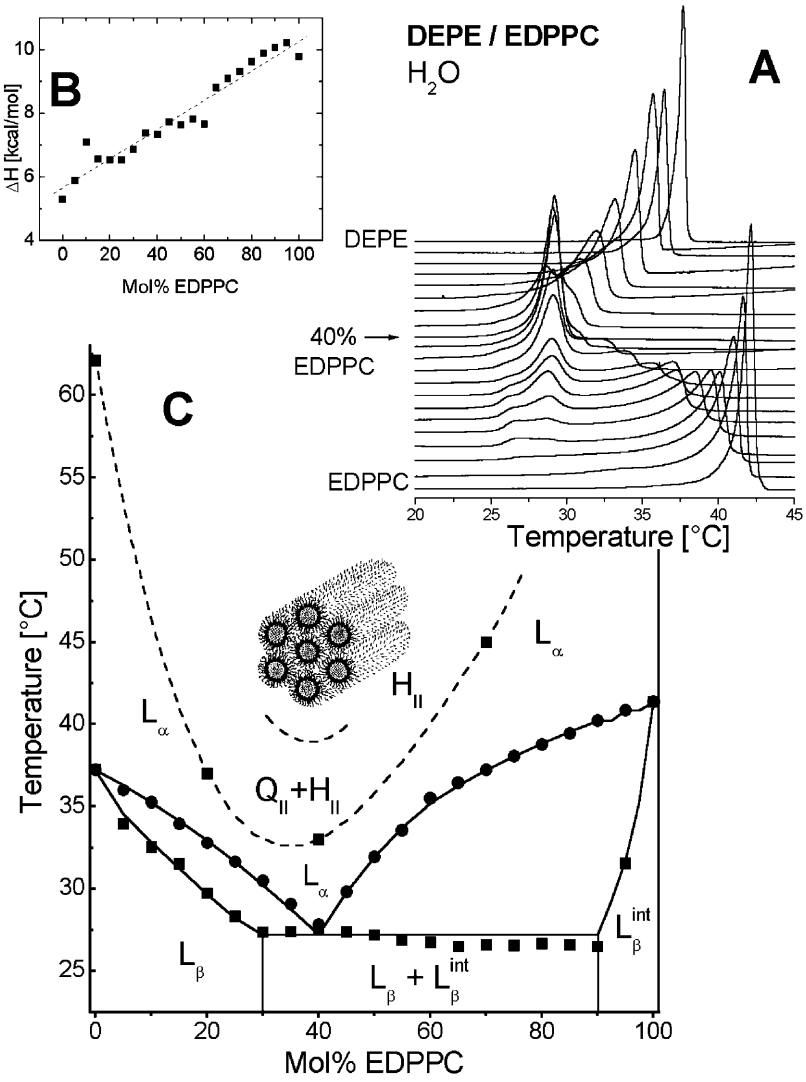

FIGURE 6 DEPE/EDPPC mixtures in water. (*A*) DSC thermograms of samples of different composition: from 100 mol % EDPPC (*bottom curve*) to 100 mol % DEPE (*top curve*), in steps of 5 mol %. (*B*) Melting transition enthalpy change. (*C*) Constructed phase diagram (phase identification based on SAXD, with account also taken of the calorimetric behavior).

resolution to record data during temperature scans. It was thus possible to detect and resolve phase structures existing in narrow temperature intervals. The phase identification according to these measurements is incorporated in Fig. 6 *C*. The results of the SAXD measurements agreed with the features derived from the shape of the phase diagram, and revealed some additional characteristics of the phase behavior of the system (Figs. 7 and 8).

At 20 mol % EDPPC (Figs. 7 *A* and 8 *B*), the phase sequence was the same as for the pure DEPE (Fig. 8 *A*), $L_\beta \rightarrow L_\alpha \rightarrow H_{II}$, but with the $L_\beta \rightarrow L_\alpha$ transition temperature decreased by 7°C as compared to the pure DEPE, to 30°C, and the $L_\alpha \rightarrow H_{II}$ transition temperature decreased by almost 30°C, to 36°C. At 40 mol % EDPPC (Figs. 7 *B* and 8 *C*), two gel phases coexisted at low temperature, in accord with what would be expected from the horizontal *solidus* line in the phase diagram—one regular L_β phase with lamellar repeat spacing of ~70 Å, and another, interdigitated L_β^{int} with repeat spacing of 43.5 Å. They simultaneously underwent a transition to the L_α phase at 28°C, which further evolved into the inverted hexagonal H_{II} phase at ~33°C (wide-angle x-ray diffraction data are necessary to unambiguously distinguish between gel and liquid crystalline lamellar phases; because of the lack of such data, here we use DSC and SAXD results in combination for phase identification). Just before the $L_\alpha \rightarrow H_{II}$ transformation, a set of reflections at rather low angles appeared in parallel with the L_α phase. Their Bragg spacings (162 Å, 132 Å), in ratio $\sqrt{2}:\sqrt{3}$, are consistent with the cubic Pn3m phase. (These two reflections are certainly not sufficient for unambiguous identification of the cubic aspect, but inasmuch as the Pn3m phase is the only one previously observed in lipid-water systems, consistent with that reflection ratio, we tentatively assign the phase as Pn3m.) That phase was observed only over 1–2°C (32–33°C). At higher temperatures, it converted into another cubic phase, with reflection spacings in the ratio $\sqrt{2}:\sqrt{4}:\sqrt{6}$, consistent with the Im3m phase (Fig. 10). At the Pn3m→Im3m transition point, the ratio of the lattice parameters of the two phases, Im3m/Pn3m, was close to 1.28, as expected theoretically according to the representa-

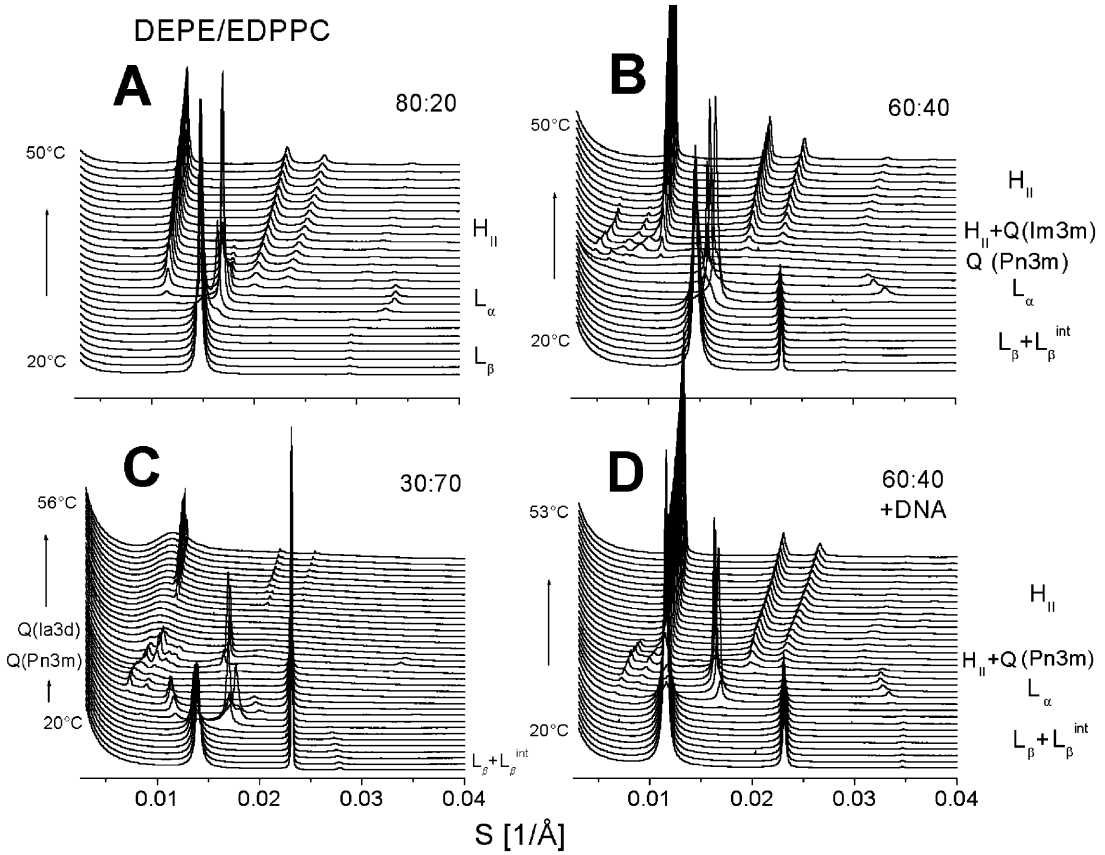

FIGURE 7 DEPE/EDPPC mixture. SAXD patterns at molar ratios of (*A*) 80:20, (*B*) 60:40, (*C*) 30:70, and (*D*) 60:40 + isoelectric amount of DNA, recorded upon heating at 1°C/min. Exposure time, 2 s.

tion of the lipid cubic phases as infinite periodical minimal surfaces, related by Bonnet transformation (a transformation of one minimal surface into another proceeding with no change in curvature; see Hyde et al., 1984; Longley and McIntosh, 1983; Seddon, 1990; Seddon and Templer, 1995; Charvolin and Sadoc, 1996). That Im3m→Pn3m conversion took place nearly simultaneously with the transformation of the lamellar L_α phase into an inverted hexagonal H_{II} phase (Figs. 7 *B* and 8 *C*). The cubic phase coexisted with the H_{II} phase up to ~40°C.

At 70 mol % EDPPC (Figs. 7 *C* and 8 *D*), as expected from the phase diagram shape, a variety of coexisting phases were observed, starting with two gel phases at low temperatures—interdigitated and noninterdigitated—as in the case of the 40 mol % sample, but at different proportions, with L_β^{int} being most prevalent. Upon entering the solid-liquid coexistence region at 28°C, the interdigitated gel phase initially coexisted with an L_α phase, then with an H_{II} phase. The latter was replaced by a cubic Pn3m phase (spacings at $\sqrt{2}$:$\sqrt{3}$:$\sqrt{4}$ ratio) at higher temperature. At even higher temperature, a cubic→cubic transformation took place. The new phase was characterized by reflections at 97.6 Å and 84.5 Å, fitting the ratio $\sqrt{6}$:$\sqrt{8}$, consistent with an Ia3d cubic phase having a 239 Å lattice parameter. The Pn3m:Ia3d lattice parameter ratio was close to 1.58, again in agreement with the description of the lipid cubic phases as periodic minimal surfaces exhibiting a Bonnet transformation. After complete melting into a disordered, highly swollen lamellar phase, the sample exhibited a transition into the H_{II} phase at 45°C (Fig. 7 *C*).

Addition of an isoelectric amount of DNA to the mixtures did not significantly change the phase diagram. It was again of the eutectic type, with a eutectic point at 45 mol % EDPPC and 30°C, and a horizontal *solidus* portion between ~35 and 85 mol % EDPPC (Fig. 9). At 20 mol % EDPPC, the phase sequence, $L_\beta \rightarrow L_\alpha \rightarrow H_{II}$, was not changed by the presence of DNA. At 40 mol % EDPPC, the phase sequence was (L_β + L_β^{int})→L_α→Q(Pn3m)→H_{II} (Figs.7 *D* and 8 *E*). The presence of DNA suppressed the transformation of the Pn3m cubic phase into Im3m, so that the Pn3m phase coexisted with the H_{II} phase up to 37°C (Fig. 10). At 70 mol % EDPPC, the H_{II} phase no longer formed in the presence of DNA, at least up to 80°C (not illustrated).

Thus, some noteworthy differences in the structural organization of the system were induced by the presence of DNA. First, when it was added to the mixed DEPE/EDPPC (60:40) bilayers, for which phase separation of aggregates with DEPE/EDPPC ~2:1 molar ratio and of

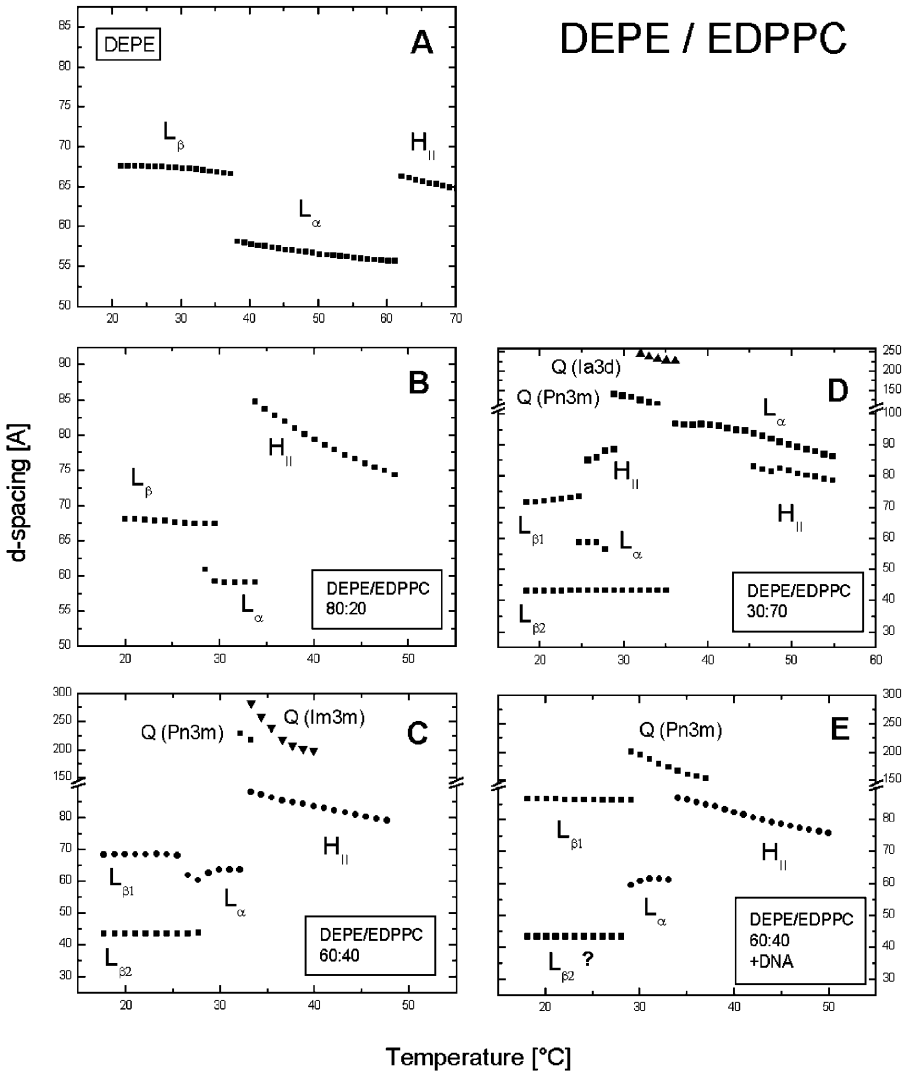

FIGURE 8 DEPE/EDPPC mixture. Variations of the SAXD spacings of the different phases formed in DEPE (*A*), and in DEPE/EDPPC mixtures at molar ratios of (*B*) 80:20, (*C*) 60:40, (*D*) 30:70, and (*E*) 60:40 + isoelectric amount of DNA, as a function of temperature. For the H_{II} phase, the position (*10*) of the diffraction peak is shown; for the cubic (Pn3m) phase, the position (*110*) of the peak is shown.

almost pure EDPPC occurred at low temperatures, DNA became incorporated into the former structures, increasing their repeat distance at 20°C by ~18 Å, from 68.5 Å to 86.6 Å (Figs. 7 *D* and 8 *E*). The existence of interdigitated bilayers of nearly pure EDPPC could not be verified because its first-order reflection (43.3 Å in the absence of DNA) coincided with the second order of the expanded mixed lamellar phase. The existence of bilayers of nearly pure EDPPC with incorporated DNA was certainly not observed in the sample—although, according to our previous experiments, their lamellar spacing is ~57 Å, and such reflection was not observed on the DEPE/EDPPC (60:40) + DNA gel phase patterns (Fig. 7 *D*). Upon heating the lipid sample with the eutectic composition (no DNA), the cubic Pn3m phase formed initially (at 32°C), and then evolved into the Im3m phase at 33°C. The latter phase was characterized with an initially rather large lattice parameter (~300 Å; Figs. 7 *B* and 8 *C*) that subsequently shrank to ~200 Å at higher temperatures. Such thermal behavior is usual for the Im3m cubic phase in lipid dispersions. If DNA was present, however, the Pn3m cubic phase formed at virtually the same temperature on heating, but it did not transform into the Im3m phase, and retained a lower lattice parameter (~200 Å at 30°C, shrinking to ~150 Å at 37°C), with less pronounced thermal contraction. One could speculate that DNA was incorporated into the complicated topology of the cubic phase, and electrostatically restricted the size of its structural node, thus preventing the Pn3m→Im3m transformation. Such a possibility is shown in Fig. 10 *D*. The H_{II} phase also had a lower structural parameter in the presence of DNA (compare to 80.0 Å at 45°C in the presence of DNA, Fig. 8 *E*, vs. 82.4 Å without DNA, Fig. 8 *C*).

The enhanced propensity of mixtures of anionic/cationic lipids to form nonlamellar phases was previously reported (Tarahovsky et al., 2000; Lewis and McElhaney, 2000). The DEPE/EDPPC mixture presents another example of a zwitterionic/cationic lipid mixture in which the initial nonlamellar propensity of DEPE is strongly enhanced by the presence of the cationic EDPPC. This is clearly interesting from the viewpoint of the possible phases induced by the

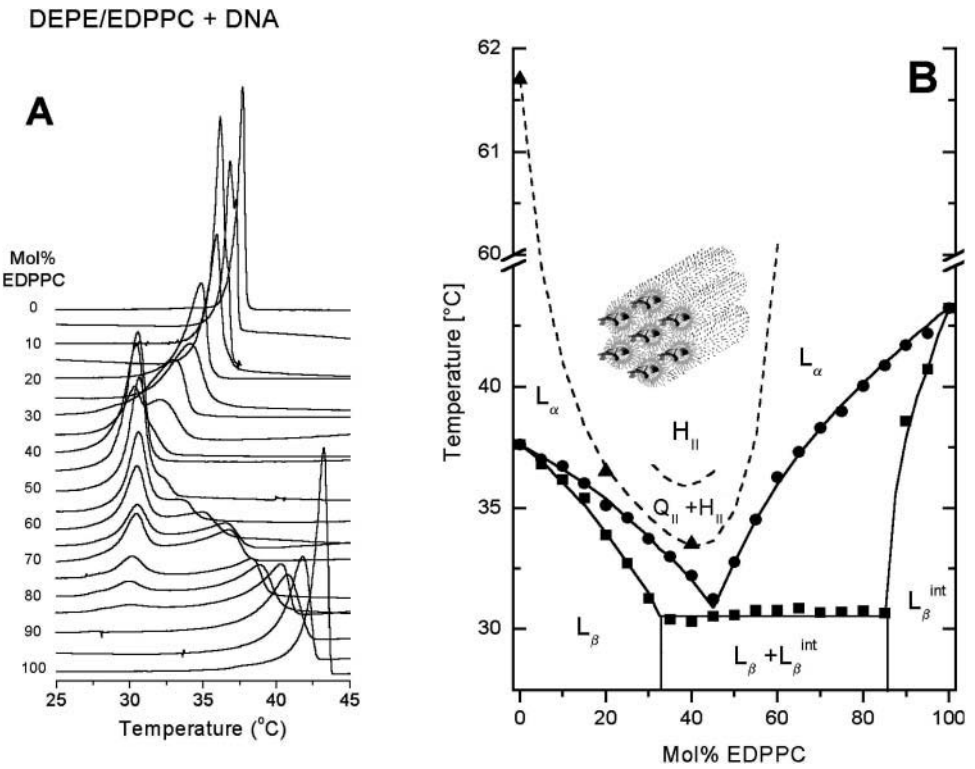

FIGURE 9 DEPE/EDPPC mixture in the presence of an isoelectric amount of DNA. (*A*) DSC thermograms recorded at 0.5°C/min heating rate; (*B*) phase diagram as constructed from the DSC data.

lipoplexes in the cellular lipid structures, but it could also have implications for transfection. It has been suggested that, at least in some cases, the H_{II} phase enhances the transfection efficiency of lipoplexes, so the DEPE/EDPPC mixture, and especially the 60:40 molar ratio preparation in which the nonlamellar phases form below the body temperature, could be a promising lipoplex candidate. Moreover, the bicontinuous cubic phase has been observed in that mixture even in the presence of DNA, and since the effect of the cubic phase topology on the transfection activity has not been examined, the DEPE/EDPPC mixture provides a noteworthy opportunity in this respect.

DPPG/EDPPC

A set of DSC thermograms of EDPPC/DPPG mixtures at different lipid ratios, dispersed in PBS, pH 7.2, are shown at Fig. 11 *A*; the derived phase diagram, corrected for the finite width of the pure component phase transitions, is depicted in Fig. 11 *B*. It is a complex phase diagram with a number of unusual aspects. At 20 mol % DPPG, an upper isoconcentration point was observed at 41°C (Fig. 11 *B*). The horizontal portion of the *solidus* line at 39.5°C between ~28 and 95 mol % DPPG corresponds to a gel phase miscibility gap in this composition range. A eutectic mixture formed at ~33 mol % DPPG. At that composition, the coexisting gel phases of ~28 and 95 mol % DPPG melted quasi-isothermally into a homogeneous liquid crystalline phase at 39.5°C. At higher DPPG concentrations, a limited region of liquid-liquid phase separation was apparent in the temperature region 41.6–43.7°C for DPPG fractions between 40 and 95 mol %.

According to the derived phase diagram, DPPG and EDPPC mix well at low DPPG concentrations, up to ~25–30 mol % at physiological conditions. It appears that the contacts between unlike molecules are preferred in the gel phase in this composition range. At higher contents of DPPG, phase separation in the gel phase and in a limited region of the liquid crystalline phase are likely. Liquid crystalline phase immiscibility is rare for lipid systems. Its occurrence in the mixtures involving cationic ethylphosphatidylcholine is noteworthy since it may be relevant for transfection.

X-ray diffraction patterns of samples at 0, 20, 33, 50, and 80 mol % DPPG recorded in real-time upon continuous temperature ramps supported the predictions based on the analysis of the phase diagram shape and added some further details. At 20 mol % DPPG (Fig. 12 *A*), the system was homogeneous over the entire temperature range examined (20–80°C). It formed an interdigitated gel phase ($d = 43.8$ Å) which melted at ~41°C into a highly swollen liquid crystalline phase ($d = 125$ Å at 42°C). This phase exhibited considerable thermal compression and shrank to $d = 93.5$ Å at 50°C. At that temperature it converted to an inverted hexagonal phase with the (10) reflection at 81 Å. The last transition was not observed calorimetrically, presumably because of a rather low enthalpy. The highly swollen, poorly-correlated lamellae possibly transformed into the

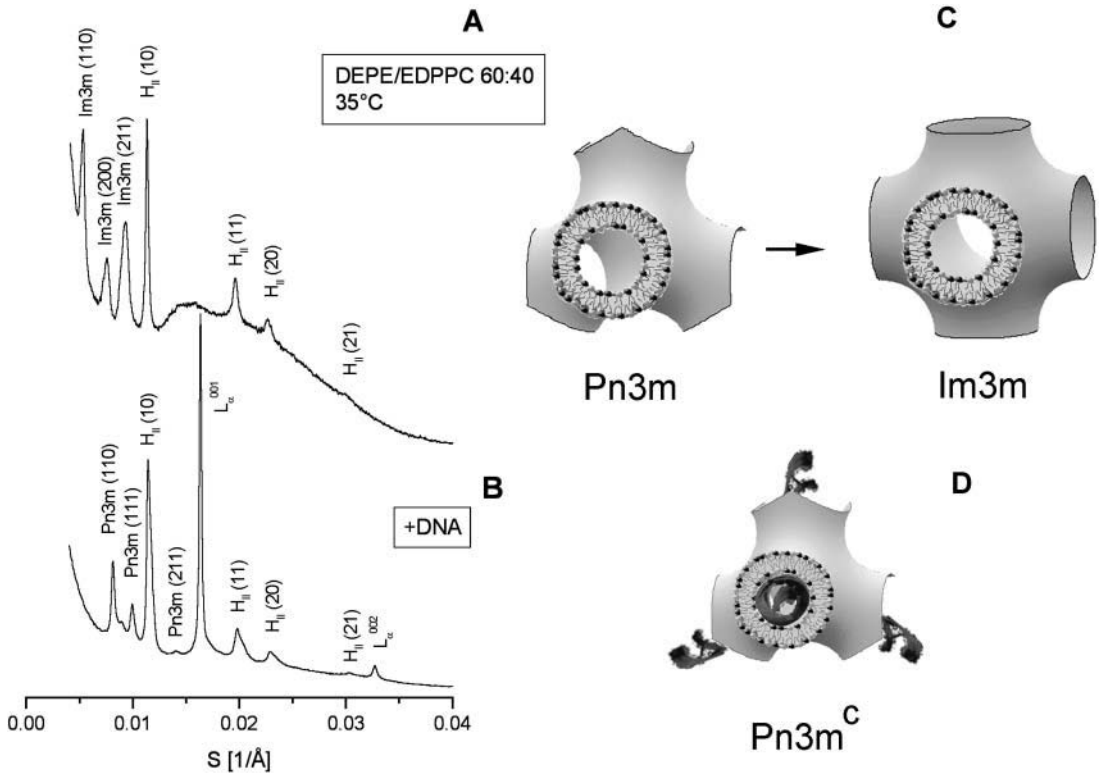

FIGURE 10 Cubic phases in the DEPE/EDPPC 60:40 sample (eutectic composition). (*A*) Diffraction pattern at 35°C exhibiting coexisting *Q* (Im3m) and H_{II} phases. (*B*) Diffraction pattern at the same temperature from a sample containing isoelectric amount of DNA, exhibiting coexisting L_α, *Q* (Pn3m), and H_{II} phases. (*C*) Cartoon representation of the bicontinuous Pn3m and Im3m cubic phases. (*D*) Cartoon representation of a complex Pn3m phase including DNA helices. Bicontinuous surfaces for the cartoons are produced using the Surface Evolver program (Brakke, 1996).

hexagonal phase much easier than well-ordered lamellar stacks, for which $L_\alpha \rightarrow H_{II}$ enthalpies of the order of a few hundreds of calories per mole are typical. Additionally, there was an excellent epitaxial correspondence between the L_α and H_{II} phases at the temperature of their interconversion: the lattice parameter of the H_{II} phase, $a = 2d/\sqrt{3}$, exactly matched the lamellar spacing of the L_α phase at the transition point, which made it conceivable that the $L_\alpha \rightarrow H_{II}$ transition proceeded without observable enthalpy change. Such an exact epitaxial match was observed not only with the 20 mol

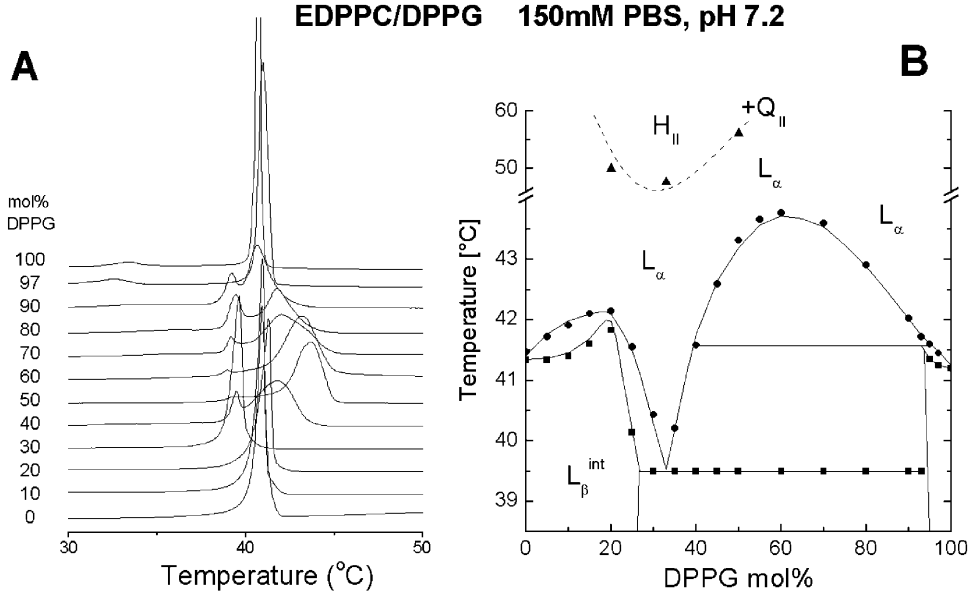

FIGURE 11 DPPG/EDPPC mixture in PBS. (*A*) DSC thermograms recorded at 0.5°C/min heating rate. (*B*) Phase diagram as constructed from the DSC data. Phase identification is from the SAXD data.

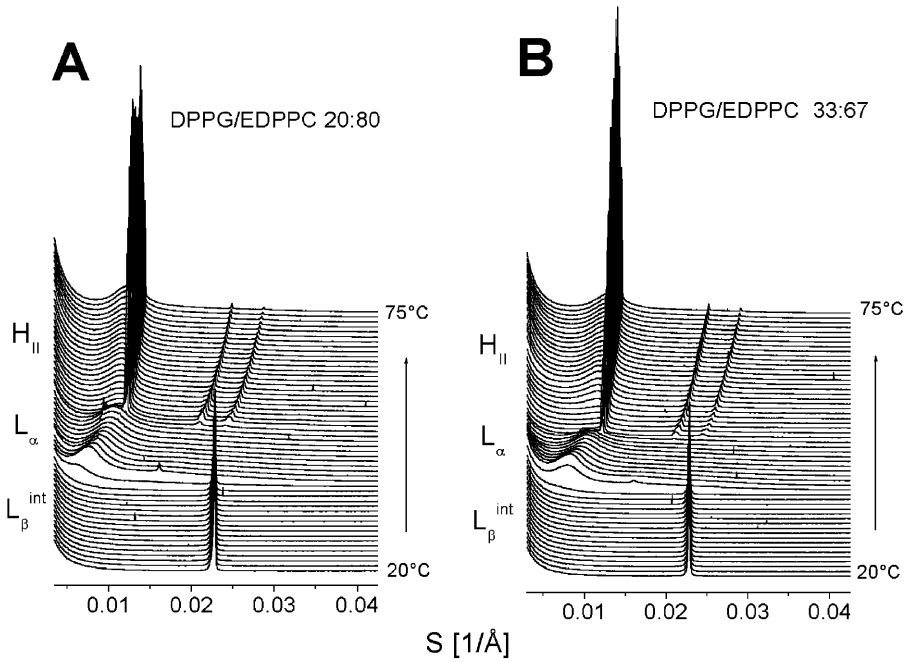

FIGURE 12 DPPG/EDPPC mixture in PBS. (*A*) SAXD patterns at molar ratios of 20:80, and (*B*) 33:67, recorded during heating at 1°C/min. Exposure time, 2 s.

% DPPG sample, but also with the 33 mol % DPPG sample (Fig. 12 *B*), in which a swollen lamellar phase with $d = 94.2$ Å converted into the H_{II} phase with a major (10) reflection of 81.6 Å at 47°C. The transition was also not observed calorimetrically in that mixture. Similarly, transformations between bicontinuous cubic phases in lipid systems, which typically take place with close epitaxial match (Tenchov et al., 1989), are sometimes (almost) not observable calorimetrically (Funari et al., 1996). The exactly commensurate L_α and H_{II} phase lattices in the DPPG/EDPPC mixtures at the $L_\alpha \rightarrow H_{II}$ transition are worth drawing attention to, since such a match is hardly observed in lipid systems (Rappolt et al., 2003).

In the 50 mol % DPPG sample, several different kinds of phase separation were observed upon heating (Fig. 13)—two lamellar gel phases at low temperature, gel, and liquid crystalline lamellar phases at intermediate temperature, and two liquid crystalline lamellar phases in a narrow temperature interval, as anticipated from the phase diagram. At higher temperatures, H_{II} and cubic (Pn3m) phases coexisted (Fig. 13, *inset*), while finally, at >70°C, only the H_{II} phase remained. At 80 mol % DPPG, nonlamellar phases were not detected at temperatures up to 75°C (not illustrated).

The DPPG/EDPPC phase diagram in water is shown in Fig. 14 *A*. The major difference from the phase diagram in salt solution (Fig. 11 *B*) is the lack of phase separation regions, presumably due to the lack of the charge screening by salts, thus rendering the segregation of like molecules more unfavorable. Still, some tendency to clustering of like molecules in the gel phase probably exists at dominant EDPPC compositions, as suggested by the lower isoconcentration point at ~33 mol % DPPG. At higher DPPG contents, the existence of an upper isoconcentration point in the phase diagram implies that the nearest-neighbor pairs in the gel phase tend to be made up of unlike molecules. Addition of an isoelectric amount of DNA did not change appreciably the phase diagram in water, especially at dominating DPPG contents (Fig. 14 *B*); the effect of DNA is mainly seen on the left side of the phase diagram, when the positive lipid charge predominates. A probable reason for this is a stronger affinity of the cationic lipid for the anionic lipid than for DNA, as could be expected because of hydrophobic interactions, which are not possible with DNA. This finding is also consistent with the observation that addition of anionic lipid to preformed lipoplexes usually results in displacement of the DNA from the lipoplexes and DNA release (Xu and Szoka, 1996; Cornelis et al., 2002). Such phenomena are important from the viewpoint of cationic lipid applications in transfection—a higher affinity of ethylphosphatidylcholines for the anionic lipid than to DNA would facilitate DNA release upon contact of lipoplexes with cell membranes.

It has been suggested for another PG/cationic lipid mixture (POPG/DOTAP), that the propensity to form inverted nonlamellar phases is maximum in mixtures where the mean surface charge of the membrane surface approaches neutrality (Lewis and McElhaney, 2000). Here we observe maximum tendency for nonlamellar phase formation at ~2:1 positive/negative charge ratio. Clearly, surface charge is only one of the parameters in the delicate balance of forces modulating the lipid phase preferences.

Cholesterol/EDPPC

Cholesterol is another membrane lipid representative, which has attracted a lot of attention in the recent years because of its suggested role in membrane rafts. Similarly to other

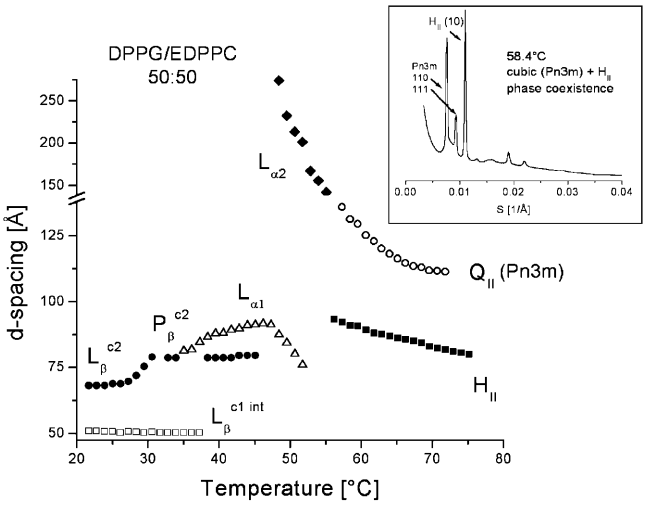

FIGURE 13 SAXD spacings of the phases in DPPG/EDPPC (50:50) mixture in PBS as a function of temperature as determined from a heating ramp at 1°C/min. For the H_{II} phase, the position (*10*) of the diffraction peak is shown; for the cubic (Pn3m) phase, the position (*110*) of the peak is shown. (*Inset*) SAXD patterns illustrating the Q(Pn3m) + H_{II} phase coexistence at 58.4°C.

phosphatidylcholine systems (Ipsen et al., 1987; Koynova et al., 1985; Vist and Davis, 1990; Nielsen et al., 1999), addition of cholesterol to EDPPC eliminated its gel-liquid crystalline phase transition (Fig. 15 *A*), which indicates the existence of a critical point in the phase diagram. With the cholesterol/EDPPC mixture, the melting transition was no longer observable on the DSC thermograms at cholesterol concentrations >50 mol %. The mixture with 30 mol % cholesterol exhibited the lowest transition temperature and was assumed to correspond to a eutectic point at the phase diagram (Fig. 15 *B*). The horizontal portion of the *solidus* line progressing to ~35 mol % cholesterol is suggestive of the formation of 2:1 EDPPC/cholesterol stoichiometric complexes at low temperatures.

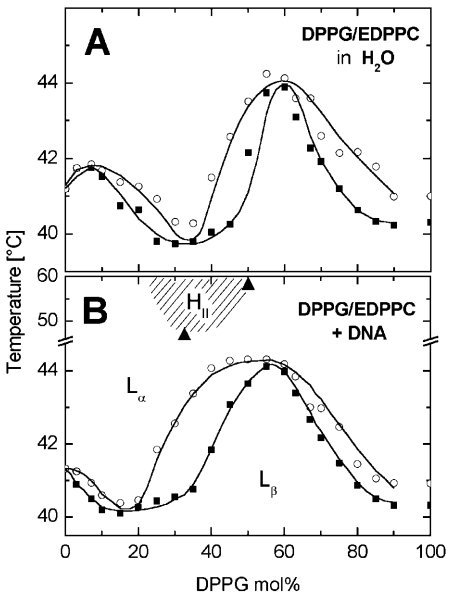

FIGURE 14 Phase diagrams of the DPPG/EDPPC binary in (*A*) H_2O, and (*B*) in the presence of isoelectric amount of DNA, constructed from DSC heating thermograms recorded at 0.5°C/min. Main transition onset (*solid squares*) and completion (*open circles*) are indicated. On the latter phase diagram, the temperatures of the $L_{\alpha} \rightarrow H_{II}$ transition in the samples with 33 mol % and 50 mol % DPPG, as determined from SAXD, are indicated (*triangles*).

SAXD patterns of cholesterol/EDPPC samples at 5 mol % and 30 mol % cholesterol, recorded during continuous temperature ramps, are shown in Fig. 16, *A* and *C*. The structural parameters of the lipid phases determined from these patterns are included in Fig. 16, *B* and *D*. At 5 mol % cholesterol, the sample converted from interdigitated lamellar gel phase (d = 43 Å at 20°C) to lamellar liquid crystalline phase (d = 53 Å at 40°C), via ~2°C phase coexistence range, upon heating (Fig. 16, *A* and *B*). A highly swollen, disordered lamellar phase also formed at higher temperatures. Complex formation and phase demixing in the gel phase was verified by the SAXD data for the 35 mol % cholesterol mixture (Fig. 16, *C* and *D*). Two lamellar phases coexisted at low temperatures—one of a short repeat distance (43 Å) typical for the interdigitated EDPPC bilayers, and another one of 60 Å lamellar spacing, typical for a regular, noninterdigitated lamellar phase, presumably formed at ~2:1 EDPPC/cholesterol stoichiometry, corresponding to the right end of the horizontal portion of the *solidus* line in the phase diagram (Fig. 15 *B*). Interestingly, the potent effect of cholesterol in eliminating chain interdigitation in DHPC bilayers has been previously reported (Laggner et al., 1991)—even 0.1 mol % cholesterol substantially perturbs interdigitation and produces coexisting interdigitated and noninterdigitated arrays, whereas 5 mol % cholesterol is enough to eliminate completely the interdigitated gel phase and to convert it into normal gel phase. With EDPPC, in contrast, 5 mol % cholesterol did not perturb the interdigitated gel phase in a detectable way, and at 30 mol % cholesterol, L_{β}^{int} still existed in parallel with the noninterdigitated phase. This difference in the effect of cholesterol on the chain interdigitation presumably reflects the different origin of this specific chain arrangement in DHPC and EDPPC aggregates; whereas, in DHPC, it is probably produced by the large mismatch between the headgroup cross-sectional area and that of the hydrocarbon chains, in EDPPC there is additional preference for that arrangement due to the electrostatic repulsion.

The two coexisting gel phases in the 30 mol % cholesterol sample simultaneously exhibited a transition to the L_{α} phase at 37°C. At higher temperatures, this L_{α} phase was replaced by an inverted hexagonal phase. Its d-spacing was 68 Å at 60°C (Fig. 16 *D*). Remarkably, the formation of the H_{II} phase in that mixture was preserved in the presence of an isoelectric amount of DNA. In fact, two H_{II} sets of reflections were discernible, one with the same spacing as in the sample without DNA, and another one with smaller spacing (63.8 Å

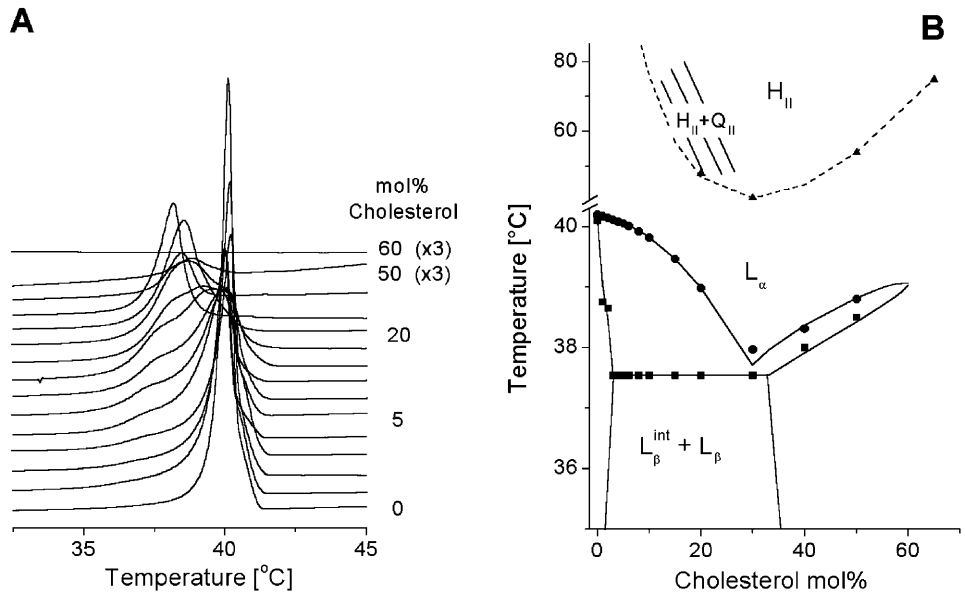

FIGURE 15 Cholesterol/EDPPC mixture in PBS. (*A*) DSC heating thermograms (0.5°C/min heating rate). (*B*) Temperature-composition phase diagram.

at 60°C) (Fig. 17). It is tempting to speculate that one of the two H_{II} phases contains DNA and the other does not (Fig. 17), and that the contraction of the unit cell of the second H_{II} phase is induced electrostatically by the presence of DNA. At 20 mol % cholesterol, traces of cubic phase were also evident in the temperature region close to the $L_\alpha \rightarrow H_{II}$ transition.

Coexisting H_{II} phases with and without DNA have also been reported in cationic liposomes prepared from mixtures of DOTAP and DOPE (Koltover et al., 1998). It has been suggested that the H_{II} phase is superior to the lamellar with regards to the transfection efficiency, at least in that lipoplex system. Here, for the first time, the formation of the H_{II} phase

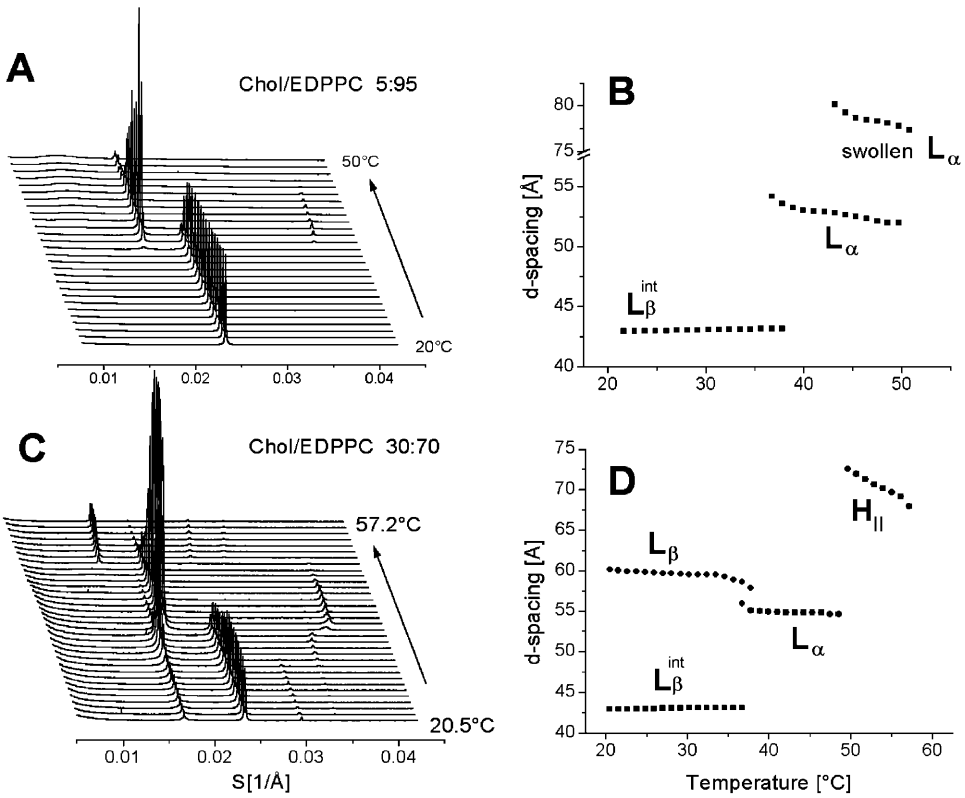

FIGURE 16 Cholesterol/EDPPC mixture. SAXD patterns of samples of (*A*) 5:95 and (*C*) 30:70 molar ratios, and (*B*, *D*) the corresponding *d*-spacings variations. For the H_{II} phase on *D*, the position (*10*) of the diffraction peak is shown.

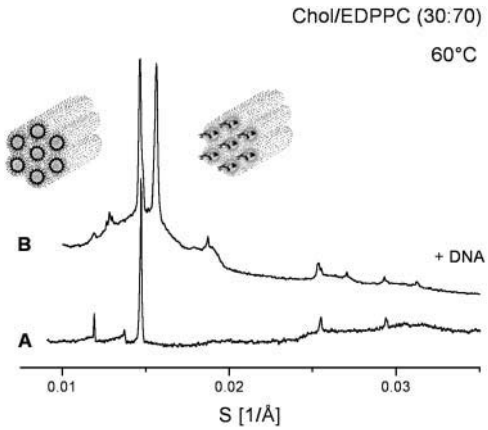

FIGURE 17 SAXD patterns of cholesterol/EDPPC (30:70, mol/mol). (*A*) Aqueous dispersion, and (*B*) in the presence of an isoelectric amount of DNA, recorded at 60°C.

is reported in a cationic lipid/cholesterol lipoplex. Although in the system we studied, the H_{II} phase forms at higher temperatures (~41°C) than appropriate for application in living systems (except perhaps for hyperthermic applications), its appearance at a temperature that low underscores nonlamellar phase propensity in the ethylphosphatidylcholine/cholesterol lipoplexes. This phenomenon is definitely worth further exploration. Moreover, the cholesterol/EDPPC lipoplexes of eutectic composition are expected to be in the vicinity of the lamellar→nonlamellar transformation at physiological temperatures, which may well affect their physical properties and their interactions with biomembranes. Since cholesterol is also a major cellular lipid, these results parallel those described above with phospholipids and further support the likelihood that a large variety of mesomorphic structures may appear after lipoplex delivery to cells. Small variations in the lipid composition may result in major differences in the structures formed in transfected cells and thus could provide a useful tool for rationalizing and even modulating transfection efficiency.

CONCLUSIONS

The hydrated binary lipid mixture DPPC/EDPPC is homogeneous at all compositions. In physiological saline, its temperature-composition phase diagram is of the lower isoconcentration point type. Simulation of the phase diagram within the regular solution approximation suggests a tendency to clustering in the gel phase and near-ideal mixing in the liquid crystalline phase. The major disparity in the gel phase packing arrangements of the two lipids—interdigitated vs. noninterdigitated, tilted—is the presumed reason for the clustering at low temperatures, despite the electrostatic repulsion. Chain interdigitation in the gel phase, characteristic of pure EDPPC, is preserved in mixtures with up to ~70 mol % DPPC. In the absence of electrolyte, the DPPC/EDPPC phase diagram exhibits lower and upper isoconcentration points, at ~20 mol % and 65 mol % EDPPC, respectively. Its complicated shape likely reflects the delicate balance between electrostatic interactions (dominating at high charge density) tending to separate the like molecules, and steric interactions (dominating at low charge density) tending to cluster them together.

The temperature-composition phase diagram of DEPE/EDPPC mixture in physiological saline is of the eutectic type, with a eutectic point at 40 mol % EDPPC and 27°C. Phase separation between aggregates of 30 mol % and 90 mol % EDPPC takes place in the gel phase at intermediate EDPPC contents. The reasons suggested for the phase separation are the major difference in the gel phase packing arrangement of EDPPC and DEPE as well as the different headgroups. At high temperatures, cubic and inverted hexagonal mesomorphic phases form over a wide compositional range. Three different cubic topologies—Pn3m, Im3m, and Ia3d—were distinguished at different lipid compositions and temperatures. The propensity to form nonlamellar phases is highest at the eutectic composition, at which the lamellar→nonlamellar transition temperature displays a minimum (33°C). The transformation follows a $L_\alpha \rightarrow Q_{II}$ (Pn3m)$\rightarrow Q_{II}$ (Im3m)$\rightarrow H_{II}$ sequence. Addition of an isoelectric amount of DNA to the mixtures suppresses the formation of the Im3m cubic phase, and also the formation of H_{II} phase at high EDPPC content. Bicontinuous lipid cubic phase formation in the presence of DNA is reported for the first time.

In the presence of PBS (pH 7.2), the phase diagram of the DPPG/EDPPC binary mixture is complicated, with several peculiar points. The two lipids mix well at low DPPG concentrations, up to ~25–30 mol %. At DPPG content >30 mol %, the system exhibits phase separation regions of the solid-solid, solid-liquid, and liquid-liquid types. Nonlamellar liquid crystalline phases (inverted hexagonal, cubic) then form, with the lowest temperature (47°C) lamellar →nonlamellar transformation occurring at 2:1 EDPPC/DPPG stoichiometry. In the absence of electrolytes, the phase separation in the mixture is not observed.

Addition of an isoelectric amount of DNA does not significantly change the DPPG/EDPPC phase diagram in water. This is taken to indicate that the lipid-lipid affinity is stronger than the cationic lipid-to-DNA affinity. Such interactions should be important for transfection and can explain DNA release upon contact of lipoplexes with cell membranes.

The cholesterol/EDPPC phase diagram exhibits a eutectic point at 30 mol % cholesterol. Coexistence of interdigitated and noninterdigitated low-temperature lamellar phases is observed at as high as 30 mol % cholesterol. With the eutectic composition, the L_α phase is least stable—an H_{II} phase forms at lowest temperature (at 41°C). Formation of a second H_{II} phase with a slightly smaller structural unit is observed in the presence of DNA.

All four mixtures exhibit a tendency to molecular clustering in the gel phase, presumably due to the specific interdigitated molecular arrangement of the EDPPC gel bilayers. With the EDPPC/dielaidoylphosphatidylcholine, EDPPC/dipalmitoylphosphatidylglycerol, and EDPPC/cholesterol mixtures, this tendency results in phase separation in the gel phase and eutectic points in their phase diagrams. Clearly, the difference of the headgroups in the last three mixtures is an additional reason for the contacts between like molecules to be preferred.

Marked enhancement of the affinity for formation of nonlamellar phases is observed in mixtures of the cationic ethylphosphatidylcholine with phosphatidylethanolamine and cholesterol as well as phosphatidylglycerol. Because of the potential relevance to transfection, it is noteworthy that such phases form at close to physiological conditions, and in the presence of DNA.

The composition with the strongest nonlamellar phase-forming tendency is different for different systems.

Cubic phase-containing lipoplexes are reported for the first time; effects on transfection are yet to be established.

In the present study, a large variety of phases have been found to form in mixtures of the cationic ethylphosphatidylcholine with representatives of cellular lipid classes. Although in multicomponent systems such as biomembranes the phase behavior could hardly be expected to match that of the binary mixtures studied here, it is still conceivable that a similarly broad array of lipid phases could arise in transfected cells. Their potential effect on the function of biomembranes needs to be carefully considered.

We acknowledge the use of the high-sensitivity DSC instrument (VP-DSC) in the Keck Biophysics Facility at Northwestern University. We are indebted to Katharina Spiegel, Director of the Keck Biophysics Facility, for assistance. Synchrotron x-ray measurements were performed at the DuPont-Northwestern-Dow Collaborative Access Team (DND-CAT) and the Biophysics Collaborative Access Team (BioCAT) Synchrotron Research Centers of the Advanced Photon Source, respectively. We are grateful to Elena Kondrashkina (BioCAT) and Steven Weigand (DND-CAT) for the assistance throughout the synchrotron experiments. We also thank Ruby MacDonald for generous help in the laboratory and for valuable discussions, and Boris Tenchov for the helpful assistance with the x-ray experiments. R.K. is grateful to Galina Chernik for expert opinion in constructing one of the phase diagrams.

This work was supported by the National Institutes of Health grant GM52329. BioCAT is an NIH-supported Research Center, through grant RR08630. DND-CAT is supported by the E. I. DuPont de Nemours and Company, The Dow Chemical Company, the U.S. National Science Foundation through grant DMR-9304725, and the State of Illinois through the Department of Commerce and the Board of Higher Education grant IBHE HECA NWU 96. Use of the Advanced Photon Source was supported by the U.S. Department of Energy, Basic Energy Sciences, Office of Energy Research under contract W-31-102-Eng-38.

REFERENCES

Bartlett, G. R. 1959. Phosphorus assay in column chromatography. *J. Biol. Chem.* 234:466–468.

Blanton, T. N., T. C. Huang, H. Toraya, C. R. Hubbard, S. B. Robie, D. Louër, H. E. Göbel, G. Will, R. Gilles, and T. Raferty. 1995. JCPDS—International Centre for Diffraction Data round-robin study of silver behenate. A possible low-angle x-ray diffraction calibration standard. *Powder Diffract.* 10:91–95.

Brakke, K. A. 1996. The Surface Evolver and the stability of liquid surfaces. *Phil. Trans. R. Soc. Lond. A.* 354:2143–2157.

Charvolin, J., and J.-F. Sadoc. 1996. Ordered bicontinuous films of amphiphiles and biological membranes. *Philos. Trans. R. Soc. Lond. A.* 354:2173–2192.

Chernik, G. G. 1995. Phase equilibria in phospholipid-water systems. *Adv. Coll. Interf. Sci.* 61:65–129.

Cornelis, S., M. Vandenbranden, J. M. Ruysschaert, and A. Elouahabi. 2002. Role of intracellular cationic liposome-DNA complex dissociation in transfection mediated by cationic lipids. *DNA Cell Biol.* 21:91–97.

Felgner, P. L., and G. M. Ringold. 1989. Cationic liposome-mediated transfection. *Nature.* 337:387–388.

Felgner, P. L. 1997. Nonviral strategies for gene therapy. *Sci. Am.* 276:102–106.

Funari, S. S., B. Mädler, and G. Rapp. 1996. Cubic topology in surfactant and lipid mixtures. *Eur. Biophys. J.* 24:293–299.

Garidel, P., C. Johann, and A. Blume. 1997. Nonideal mixing and phase separation in phosphatidylcholine-phosphatidic acid mixtures as a function of acyl chain length and pH. *Biophys. J.* 72:2196–2210.

Gordon, P. 1968. Principles of phase diagrams in material systems. McGraw-Hill, New York.

Hammersley, A. P. 1998. ESRF Internal Report, ESRF98HA01T, FIT2D V9.129. Program reference manual. V3:1.

Hammersley, A. P., S. O. Svensson, M. Hanfland, A. N. Fitch, and D. Häusermann. 1996. Two-dimensional detector software: from real detector to idealised image or two-theta scan. *High Press. Res.* 14: 235–248.

Hill, T. L. 1960. Introduction to Statistical Thermodynamics. Addison-Wesley, Reading, MA.

Hyde, S., S. Andersson, B. Ericsson, and K. Larsson. 1984. A cubic structure consisting of a lipid bilayer forming an infinite periodic minimum surface of the gyroid type in the glyceromonooleate-water system. *Z. Krystallogr.* 168:213–219.

Inoue, T., T. Tasaka, and R. Shimozawa. 1992. Miscibility of binary phospholipid mixtures under hydrated and unhydrated conditions. I. Phosphatidic acids with different acyl chain length. *Chem. Phys. Lipids.* 63:203–212.

Ipsen, J. H., G. Karlstrom, O. G. Mouritsen, K. Wennerstrom, and M. J. Zuckermann. 1987. Phase-equilibria in the phosphatidylcholine-cholesterol system. *Biochim. Biophys. Acta.* 905:162–172.

Kim, J. T., J. Mattai, and G. G. Shipley. 1987a. Gel phase polymorphism in ether-linked dihexadecylphosphatidylcholine bilayers. *Biochemistry.* 26: 6592–6598.

Kim, J. T., J. Mattai, and G. G. Shipley. 1987b. Bilayer interactions of ether- and ester-linked phospholipids: dihexadecyl- and dipalmitoylphosphatidylcholines. *Biochemistry.* 26:6599–6603.

Koltover, I., T. Salditt, J. O. Raedler, and C. R. Safinya. 1998. An inverted hexagonal phase of DNA-cationic liposome complexes related to DNA release and delivery. *Science.* 281:78–81.

Koynova, R., A. Boyanov, and B. Tenchov. 1985. On the phase diagram of L-DPPC/cholesterol mixture. *FEBS Lett.* 187:65–68.

Koynova, R., A. Boyanov, and B. Tenchov. 1987. Gel-state metastability and nature of azeotropic points in mixtures of saturated phosphatidylcholines and fatty acids. *Biochim. Biophys. Acta.* 903:186–196.

Koynova, R., and M. Caffrey. 1994. Phases and phase transitions of the hydrated phosphatidylethanolamines. *Chem. Phys. Lipids.* 69:1–34.

Koynova, R., and M. Caffrey. 1998. Phases and phase transitions of the phosphatidylcholines. *Biochim. Biophys. Acta Rev. Biomembr.* 1376:91–145.

Laggner, P., K. Lohner, G. Degovich, K. Muller, and A. Schuster. 1987. Structure and thermodynamics of the dihexadecylphosphatidylcholine-water system. *Chem. Phys. Lipids.* 44:31–60.

Laggner, P., K. Lohner, R. Koynova, and B. Tenchov. 1991. The influence of low amounts of cholesterol on the interdigitated gel phase of hydrated DHPC. *Chem. Phys. Lipids.* 60:153–161.

Lee, A. G. 1977. Lipid phase transitions and phase diagrams. II. Mixtures involving lipids. *Biochim. Biophys. Acta.* 472:285–344.

Lee, A. G. 1978. Calculation of phase diagrams for non-ideal mixtures of lipids, and a possible non-random distribution of lipids in lipid mixtures in the liquid crystalline phase. *Biochim. Biophys. Acta.* 507:433–444.

Lewis, R. N. A. H., and R. N. McElhaney. 2000. Surface charge markedly attenuates the nonlamellar phase-forming propensities of lipid bilayer membranes: calorimetric and 31P-NMR studies of mixtures of cationic, anionic, and zwitterionic lipids. *Biophys. J.* 79:1455–1464.

Lewis, R. N. A. H., I. Winter, M. Kriechbaum, K. Lohner, and R. N. McElhaney. 2001. Studies of the structure and organization of cationic lipid bilayer membranes: calorimetric, spectroscopic, and x-ray diffraction studies of linear saturated *P-O*-ethyl phosphatidylcholines. *Biophys. J.* 80:1329–1342.

Lin H.-N. and Huang C.-H. 1988. Eutectic phase behavior of 1-stearoyl-2-caprylphosphatidylcholine and dimyristoylphosphatidylcholine mixtures. *Biochim. Biophys. Acta.* 946:178–184.

Linseisen, F. M., S. Bayerl, and T. M. Bayerl. 1996. 2H-NMR and DSC study of DPPC-DODAB mixtures. *Chem. Phys. Lipids.* 83:9–23.

Lohner, K., A. Schuster, G. Degovics, K. Muller, and P. Laggner. 1987. Thermal phase behavior and structure of hydrated mixtures between dipalmitoyl- and dihexadecylphosphatidylcholine. *Chem. Phys. Lipids.* 44:61–70.

Longley, W., and T. J. McIntosh. 1983. A bicontinuous tetrahedral structure in a liquid-crystalline lipid. *Nature.* 303:612–614.

MacDonald, R. C., G. W. Ashley, M. M. Shida, V. A. Rakhmanova, Y. S. Tarahovsky, D. P. Pantazatos, M. T. Kennedy, E. V. Pozharski, K. A. Baker, R. D. Jones, H. S. Rosenzweig, K. L. Choi, R. Qiu, and T. J. McIntosh. 1999a. Physical and biological properties of cationic triesters of phosphatidylcholine. *Biophys. J.* 77:2612–2629.

MacDonald, R. C., V. A. Rakhmanova, K. L. Choi, H. S. Rosenzweig, and M. K. Lahiri. 1999b. *O*-ethylphosphatidylcholine: a metabolizable cationic phospholipid which is a serum-compatible DNA transfection agent. *J. Pharm. Sci.* 88:896–904.

Mincheva, R., A. Boyanov, and B. Tenchov. 1990. Interaction of ''solid'' and ''liquid crystalline'' multilamellar liposomes with alveolar macrophages. *C.R. Acad. Bulg. Sci.* 43:99–100.

Nambi, P., E. S. Rowe, and T. J. McIntosh. 1988. Studies of the ethanol-induced interdigitated gel phase in phosphatidylcholines using the fluorophore 1,2-diphenyl-1,3,5-hexatriene. *Biochemistry.* 27:9175–9182.

Nielsen, M., L. Miao, J. H. Ipsen, M. J. Zuckermann, and O. G. Mouritsen. 1999. Off-lattice model for the phase behavior of lipid-cholesterol bilayers. *Phys. Rev. E.* 59:5790–5803.

Ohki, K., K. Tamura, and I. Hatta. 1990. Ethanol induces interdigitated gel phase (L_β^{I}) between lamellar gel phase (L_β') and ripple phase (P_β') in phosphatidylcholine membranes: a scanning density meter study. *Biochim. Biophys. Acta.* 1028:215–222.

Phillips, W. C., A. Stewart, M. Stanton, I. Naday, and C. Ingersoll. 2002. High-sensitivity CCD-based x-ray detector. *J. Synchr. Rad.* 9:36–43.

Plotnikov, V. V., J. M. Brandts, L.-N. Lin, and J. F. Brandts. 1997. A new ultrasensitive scanning calorimeter. *Anal. Biochem.* 250:237–244.

Rakhmanova, V. A., T. J. McIntosh, and R. C. MacDonald. 2000. Effect of dioleoylphosphatidylethanolamine on the activity and structure of *O*-alkyl phosphatidylcholine-DNA transfection complexes. *Cell. Mol. Biol. Lett.* 5:51–65.

Rappolt, M., A. Hickel, F. Bringezu, and K. Lohner. 2003. Mechanism of the lamellar/inverse hexagonal phase transition examined by high resolution x-ray diffraction. *Biophys. J.* 84:3111–3122.

Rosenzweig, H., V. A. Rakhmanova, T. J. McIntosh, and R. C. MacDonald. 2000. *O*-alkyl dioleoylphosphatidylcholinium compounds: the effect of varying alkyl chain length on their physical properties and in vitro DNA transfection activity. *Bioconjug. Chem.* 11:306–313.

Seddon, J. M. 1990. Structure of the inverted hexagonal (H_{II}) phase and non-lamellar phase transitions of lipids. *Biochim. Biophys. Acta.* 1031: 1–69.

Seddon, J. M., and R. H. Templer. 1995. Polymorphism of lipid-water systems. *In* Handbook of Biological Physics. R. Lipowsky, and E. Sackmann, editors. Elsevier Science, Amsterdam, The Netherlands. 97–160.

Silvius, J. R. 1991. Anomalous mixing of zwitterionic and anionic phospholipids with double-chain cationic amphiphiles in lipid bilayers. *Biochim. Biophys. Acta.* 1070:51–59.

Simon, S. A., and T. J. McIntosh. 1984. Interdigitated hydrocarbon chain packing causes the biphasic transition behavior in lipid/alcohol suspensions. *Biochim. Biophys. Acta.* 773:169–172.

Sisk R.B. and C.-H. Huang. 1992. Calorimetric studies on the influence of *n*-methylated headgroups on the mixing behavior of diheptadecanoylphosphatidylcholine with 1-behenoyl-2-lauroylphosphatidylcholine. *Biophys. J.* 61:593–603.

Solodin, I., C. S. Brown, and T. D. Heath. 1996. Synthesis of phosphotriester cationic phospholipids. Cationic lipids 2. *Syn. Lett.* 5:457–458.

Swamy, M. J., U. Wurz, and D. Marsh. 1995. Phase polymorphism, molecular interactions and miscibility of binary mixtures of dimyristoyl-*n*-biotinylphosphatidylethanolamine with dimyristoylphosphatidylcholine. *Biochemistry.* 34:7295–7302.

Tarahovsky, Y. S., A. L. Arsenault, R. C. MacDonald, T. J. McIntosh, and R. M. Epand. 2000. Electrostatic control of phospholipid polymorphism. *Biophys. J.* 79:3193–3200.

Tenchov, B. G. 1985. Nonuniform lipid distribution in membranes. *Prog. Surf. Sci.* 20:273–340.

Tenchov, B. G., J. G. Brankov, and R. D. Koynova. 1984. Lateral lipid-lipid interactions in DPPC/DPPE bilayers. *Studia Biophys.* 103:89–96.

Tenchov, B. G., D. N. Petsev, R. D. Koynova, C. S. Vassilieff, H. W. Meyer, and J. Wunderlich. 1989. Liposome-glass interaction: influence of lipid bilayer phase state. *Coll. Surf.* 39:361–370.

Vist, M., and J. H. Davis. 1990. Phase equilibria of cholesterol/dipalmitoylphosphatidylcholine mixtures: 2H nuclear magnetic resonance and differential scanning calorimetry. *Biochemistry.* 29:451–464.

von Dreele, P. H. 1978. Estimation of lateral species separation from phase transitions in nonideal two-dimensional lipid mixtures. *Biochemistry.* 17:3939–3948.

Winter, I., G. Pabst, M. Rappolt, and K. Lohner. 2001. Refined structure of 1,2-diacyl-*P-O*-ethylphosphatidylcholine bilayer membranes. *Chem. Phys. Lipids.* 112:137–150.

Xu, Y., and F. C. Szoka, Jr. 1996. Mechanism of DNA release from cationic liposome/DNA complexes used in cell transfection. *Biochemistry.* 35:5616–5623.

Zantl, R., L. Baicu, F. Artzner, I. Sprenger, G. Rapp, and J. O. Raedler. 1999. Thermotropic phase behavior of cationic lipid-DNA complexes compared to binary lipid mixtures. *J. Phys. Chem. B.* 103:10300–10310.

Zhu, N., D. Liggitt, Y. Liu, and R. Debs. 1993. Systematic gene expression after intravenous DNA delivery into adult mice. *Science.* 261:209–211.

Zuhorn, I. S., and D. Hoekstra. 2002. On the mechanism of cationic amphiphile-mediated transfection. To fuse or not to fuse: is that the question? *J. Membr. Biol.* 189:167–179.

Zuhorn, I. S., V. Oberle, W. H. Visser, J. B. F. N. Engberts, U. Bakowsky, E. Polushkin, and D. Hoekstra. 2002. Phase behavior of cationic amphiphiles and their mixtures with helper lipid influences lipoplex shape, DNA translocation, and transfection efficiency. *Biophys. J.* 83: 2096–2108.